

PDP: Physics-Based Character Animation via Diffusion Policy

Takara E. Truong
Stanford University
Stanford, CA, USA

Michael Pisen
Stanford University
Stanford, CA, USA

Zhaoming Xie
Stanford University
Stanford, CA, USA

C. Karen Liu
Stanford University
Stanford, CA, USA

Email: takaraet@stanford.edu Email: mpisen@stanford.edu Email: zhxie@stanford.edu Email: karenliu@cs.stanford.edu

Abstract—Generating diverse and realistic human motion that can physically interact with an environment remains a challenging research area in character animation. Meanwhile, diffusion-based methods, as proposed by the robotics community, have demonstrated the ability to capture highly diverse and multi-modal skills. However, naively training a diffusion policy often results in unstable motions for high-frequency, under-actuated control tasks like bipedal locomotion due to rapidly accumulating compounding errors, pushing the agent away from optimal training trajectories. The key idea lies in using RL policies not just for providing optimal trajectories but for providing corrective actions in sub-optimal states, giving the policy a chance to correct for errors caused by environmental stimulus, model errors, or numerical errors in simulation. Our method, Physics-Based Character Animation via Diffusion Policy (PDP), combines reinforcement learning (RL) and behavior cloning (BC) to create a robust diffusion policy for physics-based character animation. We demonstrate PDP on perturbation recovery, universal motion tracking, and physics-based text-to-motion synthesis.

Index Terms—character animation, reinforcement learning, diffusion models

I. INTRODUCTION

Developing a framework capable of generating diverse human movements that can proficiently traverse and interact with the environment is a crucial objective in character animation with broad applications in robotics, exoskeletons, virtual/augmented reality, and video games. Many of these applications demand not only a diverse range of human kinematic poses, but also the physical actions needed to achieve them. Previous works have demonstrated that physics-based control tasks can be formulated as a Markov Decision Process and solved through a Reinforcement Learning (RL) algorithm, or as a regression problem and solved using supervised learning techniques such as Behavior Cloning (BC). Despite the achievements observed in dynamic motor skills learning through both RL and BC methodologies, they encounter difficulties in effectively capturing the diversity and multi-model characteristics inherent in human motions.

To address this issue, recent works have explored various generative models. While Generative Adversarial Network (GAN) and Conditional Variational Autoencoder (C-VAE) based methods have been used to capture humanoid skills, GAN based methods can only cover a small set of skills due to mode collapse and VAE-based models suffer from sensitive trade-off between diversity and robustness. Although

diffusion models have been used to generate varied kinematic human motion [1], [2], their application to robotics is more recent. Recent robotics research shows that BC combined with diffusion models can effectively learn diverse and multi-modal actions for real-world execution [3], [4]. However, naively training a diffusion-based BC policy is ineffective for physics-based character animation due to compounding errors in high-frequency, under-actuated control tasks, exacerbating the domain shift problem. This issue is especially prominent in bipedal locomotion, where accumulated errors can quickly lead to falling. Can we combine the strengths of RL and diffusion-based BC policy, such that a physically simulated character can perform a diverse set of tasks robustly against distribution shifts due to disturbances in the environment, error in model prediction, or numerical errors in simulation?

We introduce PDP, a novel method that learns a robust diffusion policy for physics-based character animation, addressing the noted challenges. PDP leverages diffusion policies [5] and large-scale motion datasets to learn diverse and multimodal motor skills through supervised learning and diffusion models. To overcome sensitivity to domain shifts, PDP uses expert RL policies to gather physically valid sequences of observations and actions. However, using RL for data collection alone does not resolve domain shift sensitivity.

Our key insight is that RL policies provide not only optimal trajectories but more importantly corrective actions from sub-optimal states. We employ a sampling strategy from robotics literature [6], collecting noisy-state clean-action paired trajectories to train the diffusion policy. We find that the choice of pairing noisy state with clean actions is a critical detail that contributes to producing a robust policy, outperforming the standard clean-state-clean-action trajectory collection and noisy-state-noisy-action sampling strategies for domain randomization. Additionally, we can now pool together data collected by small-task RL policies which can be efficiently trained, and leave the learning of diverse tasks on large-scale datasets to supervised learning.

PDP is a versatile method applicable to various motion synthesis tasks and agnostic to training datasets. We evaluate PDP on locomotion control under large physical perturbations, universal motion tracking, and physics-based text-to-motion synthesis, using different motion capture datasets for each application. Our model captures the multi-modality of human

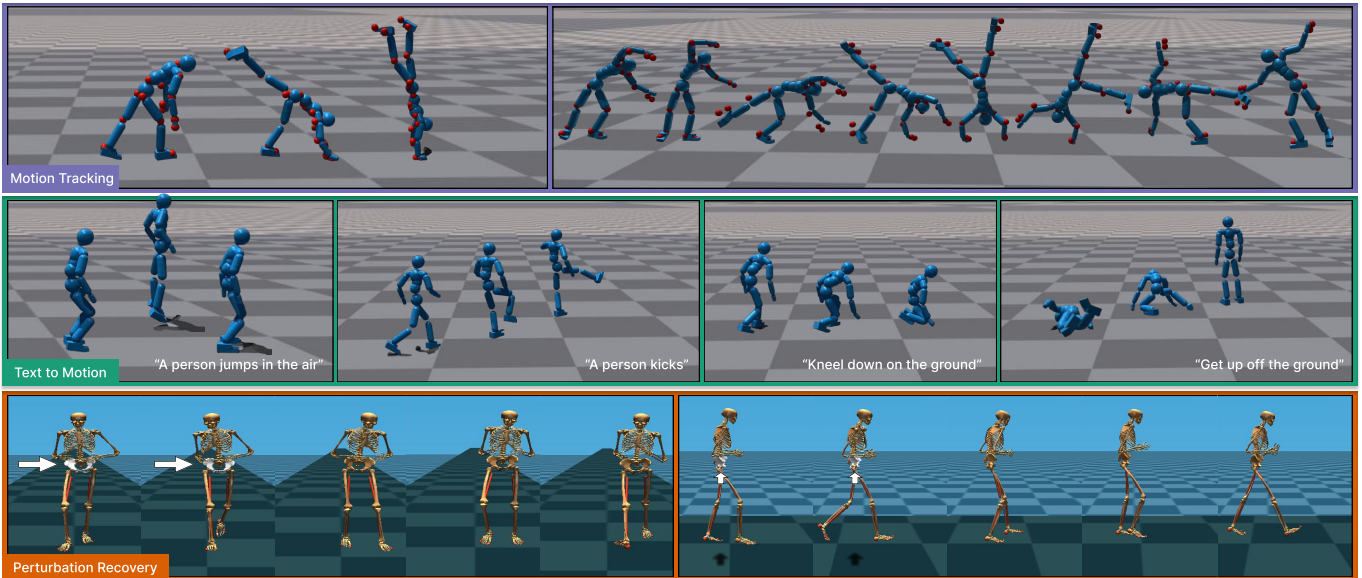


Fig. 1. PDP performs well across a diverse range of physics-based application domains. Top: Motion tracking. PDP is capable of tracking difficult and highly dynamic motions such as handstands and cartwheels. Middle: Text-to-motion. PDP is also capable of following user-provided text instructions. Bottom: Robustness to perturbations. PDP learns robust recovery strategies from random perturbations.

push recovery behavior, outperforming VAE-based methods and deterministic multi-layer perceptron networks on the bump-em dataset [7]. It can also track 98.9% of all AMASS motions and [8] generate motion from textual descriptions [9]. Our contributions are as follows:

- We present a method of robust BC that scales to large motion datasets without the need for complex training architectures and can easily adapt to new skills.
- We analyze the effect of different sampling strategies for data augmentation on model performance.
- We introduce physics-based models that support locomotion control, motion tracking, and text-to-motion tasks.

II. RELATED WORK

A. Physics-Based Character Animation via RL

In physics-based character animation, the central challenge is developing systems that can learn diverse movements and motor skills for specific tasks. This includes motion tracking, motion generation, and task-oriented applications, which require consideration of physical interactions. Proficiency in these skills is crucial for applications in gaming, virtual reality, and robotics, where authentic and adaptable movements play a vital role.

Single motion imitation using RL enables policies to imitate specific movements or skills, such as walking, running, or jumping [10]. However, these policies alone may not suffice to complete tasks that involve multiple skills. By conditioning policies on future motions, multiple skills can be learned, and a motion generator can guide the policies to complete desired tasks [11], [12]. However, learning control policies that scale to many skills is challenging. [13] proposes to use a mixture of experts, where different experts specialize in different skills.

[14] proposes an iterative approach to learning a large number of skills sequentially.

Another challenge in physics-based character animation is capturing the diversity of skills in the motion data. Human behavior is multimodal, meaning a range of plausible behaviors can be employed in the same situation, which can lead to mode collapse, where only a single behavior is learned [15]. To capture the diversity of human skills, Conditional Variational Autoencoders (C-VAE) [16]–[19] are used to learn a latent space of skills, enabling random sampling to induce a wide range of motions. [20] achieved a similar capability by combining a diversity reward and adversarial reward that encourage the policy to capture the distribution of human motion data.

Achieving the capability to scale to a large motion dataset while maintaining diversity is still a challenging problem. We propose to use the diffusion model to handle this challenge and demonstrate control policies that perform a large number of skills while maintaining diversity.

B. Diffusion Models for Motion Synthesis and Robotics

Similar to VAEs, Diffusion models represent another category of generative AI and have exhibited success in the domain of kinematic motion synthesis, showcasing the capability of generating diverse and intricate human motion patterns [1], [21]. Recently, Diffusion Policy [3] has been applied diffusion models to robotic manipulation tasks, human-robot collaborative endeavors [22], and tasks involving following language instructions [23]. These models have primarily concentrated on high-level motion planning with a limited action space, such as forecasting the end-effector trajectory. While effective in stable environments, the application of Diffusion Policy to scenarios where minor inaccuracies in model predictions could result in

failure, as observed in physics-based character animation, has only recently been explored in [4]. In contexts requiring high-frequency control, ensuring that the policy remains unaffected by domain shifts is crucial. Through our sampling technique, we have enhanced the robustness of the policy, addressing the domain shift issue and enabling the utilization of diffusion models in the character animation domain. Similar observations have been reported in concurrent studies in quadruped and bi-pedal robot domains [4].

III. METHODS

Our method consists of three stages. First, we train a set of expert policies, each specialized in a small task but together completing a wide variety of motion tracking tasks in a physics simulator. Second, we generate state-action trajectories from the trained policies stochastically to build a dataset with noisy-state and clean-action trajectories. Lastly, we train a diffusion model via Behavior Cloning (BC) to obtain a single policy that can perform all tasks. Fig. 2 depicts an overview of our method.

A. Expert Policy Training

We aim to obtain a control policy $\pi_{\text{PDP}} : \mathcal{O} \times \mathcal{T} \rightarrow \mathcal{A}$ to control a humanoid character, where \mathcal{O} is the set of observations that describes the state of the character, \mathcal{T} is the set of tasks, and \mathcal{A} is the set of actions used to control the humanoid character. Such control policies can be trained via reinforcement learning. However, when the set \mathcal{T} is large, it may be challenging to train a single policy to master all tasks, while it is relatively easy to train policies that specialize in a subset of tasks. We can divide the task set \mathcal{T} into subset $\{\mathcal{T}_1, \mathcal{T}_2, \dots, \mathcal{T}_k\}$, where $\bigcup_i \mathcal{T}_i = \mathcal{T}$, and train an expert policy $\pi_{\mathcal{T}_i}$ for each \mathcal{T}_i . The strategy for dividing the task is not critical, as long as it results in a set of policies that can generate desired state-action trajectories.

B. Stochastic Data Collection

In the second stage, we utilize the expert policies to generate a dataset for BC. For each task \mathcal{T}_i , we create a dataset $\mathcal{D}_{\mathcal{T}_i}$ by rolling out policy $\pi_{\mathcal{T}_i}$ and collecting trajectories. Specifically, we sample a motion task $\tau \in \mathcal{T}_i$, and run the policy to generate a sequence $\{\mathbf{o}_0, \mathbf{a}_0, \mathbf{o}_1, \mathbf{a}_1, \dots, \mathbf{o}_N, \mathbf{a}_N\}$, where $\mathbf{a}_t = \pi_{\mathcal{T}_i}(\mathbf{o}_t, \tau) + \epsilon$ is a noisy version of optimal action proposed by the expert policy. The tuples $(\mathbf{o}_t, \tau, \pi_{\mathcal{T}_i}(\mathbf{o}_t, \tau))$ which correspond to the observation, task/goal information, and action are added to the dataset $\mathcal{D}_{\mathcal{T}_i}$. We repeat the data collection process until a maximum number of data points are collected, and use $\mathcal{D} = \bigcup \mathcal{D}_{\mathcal{T}_i}$ as the dataset for BC. Note that the optimal action, not the noisy action \mathbf{a}_t , is stored in $\mathcal{D}_{\mathcal{T}_i}$ and can be thought of as a corrective action from a noisy observation. This important detail, inspired by the DASS strategy proposed by [6], results in a training set that consists of sequences of noisy-state and clean-action pairs. This allows the collected data to cover a wider range of observation space compared to naively collecting clean optimal state-action trajectories, effectively creating a “noise band” around the

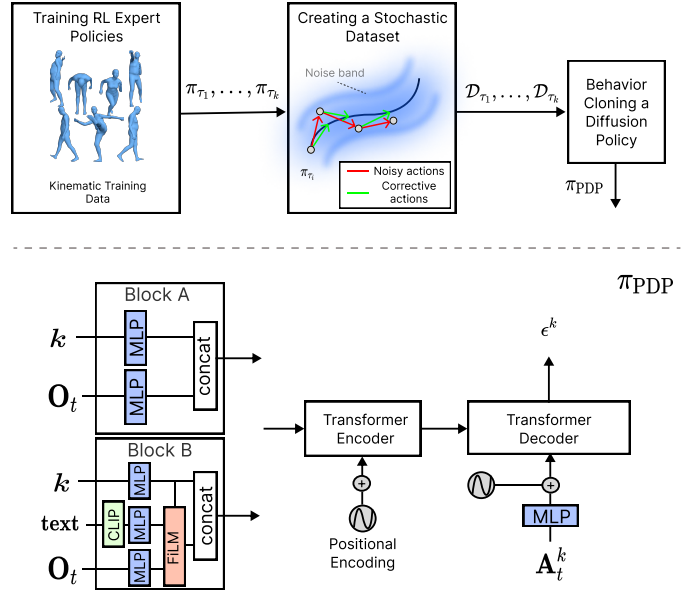


Fig. 2. PDP Overview. Top: First, we train expert RL policies $\pi_{\mathcal{T}_i}$ on tasks \mathcal{T}_i . We use $\pi_{\mathcal{T}_i}$ to create a dataset of noisy-state clean-actions. We then use BC to train a diffusion model. Bottom: Our model is a transformer encoder-decoder architecture. Block-B is used for text conditioned tasks, while all other tasks use Block A.

clean trajectories. Another potential option is to collect noisy-state and noisy-action pairs, a common domain randomization practice in robotics to battle the sim-to-real gap. We found this randomization strategy produces less robust policies for character animation.

C. Behavior Cloning with Diffusion Policy

We parameterize our policy as a diffusion model. Here we give an overview of the diffusion model and our choice of architecture.

1) *Diffusion model*: We employ Diffusion Policy [3], which models the action distribution conditioned on the observations as a denoising process using a Denoising Diffusion Probabilistic Model (DDPM) [24]. Given a dataset of sequences \mathcal{D} collected using the method described previously, the denoising process is learned by a noise-prediction network $\epsilon_{\theta}(\mathbf{A}_t^k, \mathbf{O}_t, \tau, k)$, where \mathbf{A}_t^k is an action sequence sampled from \mathcal{D} with added Gaussian noise and k is the diffusion step. The diffusion model is conditioned on \mathbf{O}_t , the corresponding observation sequence. τ is the necessary task or goal information, and θ is the set of learned model parameters. \mathbf{A}_t^k and \mathbf{O}_t are length T sequences of actions and observations beginning at episode timestep t . Sampling is then achieved through a denoising process known as Stochastic Langevin Dynamics [25] starting from pure random noise.

$$\mathbf{A}_t^{k-1} = \alpha(\mathbf{A}_t^k - \gamma \epsilon_{\theta}(\mathbf{A}_t^k, \mathbf{O}_t, \tau, k) + \mathcal{N}(0, \sigma^2 \mathbf{I})), \quad (1)$$

where α, γ and σ are hyper-parameters of the denoising process. The noise-prediction model is learned in a self-supervised manner using the mean squared error objective

$$\mathcal{L} = \text{MSE}(\epsilon^k, \epsilon_\theta(\mathbf{A}_t^0 + \epsilon^k, \mathbf{O}_t, \tau_t, k)), \quad (2)$$

where ϵ^k is the noise applied at to the action sequence at diffusion step k and \mathbf{A}_t^0 is the clean action sequence.

2) *Model Architecture*: Fig. 2 depicts our model architecture. We adopt a similar architecture to the time-series diffusion transformer proposed by Diffusion Policy [3], with slight modifications depending on the application. For locomotion control and motion tracking, task information is included in the observation. For text-to-motion, the conditioning for the action sequence is computed as follows: a raw text prompt is encoded using the CLIP ViT-B/32 model [26], then passed through an MLP text encoder. The observation \mathbf{O}_t is also fed through an MLP encoder. The diffusion step k is embedded into the same space and added to the text embedding. This result is fed through a Feature-wise Linear Modulation (FiLM) layer [27], which applies a learned element-wise scale and shift transformation to the embedding of \mathbf{O}_t . Finally, the diffusion step embedding is concatenated with the FiLM layer result to produce our condition, serving as the input to the transformer encoder. This conditioning method is represented in Block B of Figure 2. The transformer decoder then takes an embedding of the noisy action sequence \mathbf{A}_t^k along with the encoder result and predicts the noise applied to the action ϵ^k . For motion tracking tasks, we condition our transformer encoder using Block A of Figure 2, which is similar to Block B but without the CLIP text.

IV. EXPERIMENTAL DETAILS

We demonstrate the generality and effectiveness of PDP by applying it to three distinctive applications using three different datasets: locomotion control under large physical perturbations using addbiomechanics dataset [7], universal motion tracking using AMASS [8], and physics-based text-to-motion synthesis using the KIT subset of AMASS and HumanML3D [9] for text labels. Experimental details for each application are described in this section, with results, comparisons, and ablation studies presented in the next section.

A. Perturbation Recovery

The goal of the perturbation recovery task is to train a single diffusion policy that is capable of capturing the wide range of human responses to perturbations. Being able to model and simulate this behavior is important for studying human robustness [28] and for designing better exo-skeleton or prosthetic systems [29].

1) *Dataset*: We use the Bump-em dataset, a subset of the Addbiomechanics dataset [7], which consists of recovery motions of human participants being physically pushed while walking on a treadmill. Participants are perturbed in the same stance with varying forces and directions applied to the hip through a parallel tethered robot [30]. The recorded motions demonstrate that participants exhibit a diverse set of recovery

strategies even under the same perturbation and initial stance, which makes this dataset particularly well suited for studying how well a model can capture the multi-modality of human behaviour.

For this task, trials from one participant were used. Perturbations were collected as the subject walked forward on a treadmill at a fixed speed, impacted at left toe-off stance in four directions (front, left, right, back) with magnitudes of 7.5% and 15% body weight. Two trials of each configuration were collected, resulting in 16 motions for the participant. However, two were dropped due to poor motion quality resulting in a dataset of 14 motion trajectories.

2) *Experimental Details*: We use a 25-joint skeletal model from Addbiomechanics [7], optimized for the specific participant’s inertia and joint lengths. The environment is simulated with Mujoco and consists of the simulated treadmill and the skeletal model. In this environment, the observation space is defined in the world frame. The RL agent’s observation consists of the bodies center of mass positions $\mathbf{x}^p \in \mathbb{R}^{3B}$ and linear velocities $\dot{\mathbf{x}}^p \in \mathbb{R}^{3B}$, as well as the bodies rotation $\mathbf{x}^r \in \mathbb{R}^{3 \times 3 \times B}$. During RL training, the agent receives the same perturbation experienced by the human during the trial and optimizes tracking the human response through the collected reference motion following [10].

After training expert RL policies for each motion, we collect new observations for PDP, by including a binary signal \mathbf{p} that indicates if the human is being perturbed, without detailing the force magnitude or direction. This signal is helpful for the diffusion policy to differentiate between normal walking and perturbation recovery; otherwise, the policy would react to non-existent perturbations. This addition is justified, as humans can discern disturbances directly, providing no predictive advantage. The full perturbation recovery observation can then be defined as a tuple $(\mathbf{x}^p, \mathbf{x}^r, \dot{\mathbf{x}}^p, \dot{\mathbf{x}}^r, \mathbf{p})$. 14 motions were sampled using the various noisy/clean state action strategies, and used to train PDP. Each model was trained on a single RTX 2080 Ti GPU for approximately 1.5 hours.

B. Universal Motion Tracking

The goal of the universal motion tracking task is to train a single diffusion policy capable of controlling the character to track any given reference motion under physics simulation.

1) *Dataset*: We use the AMASS dataset, and use the same train/test splits as PHC [14], where the subsets “Transitions Mocap” and “SSM synced” are used for testing and the rest are placed in the training set. Since our method is agnostic to the RL policies themselves, we utilize pre-trained motion tracking controller PHC [14] to track most of the motions and train individual RL policies for challenging motions where PHC fails [10]. With PHC and a few specialized small policies, our expert policies produce a training set that covers most motions in AMASS [8] and KIT [31]. Following the same practice in PHC, we exclude motions that are infeasible in our physics simulators, such as leaning on tables.

2) *Experimental Details*: We use the humanoid model from [14], which follows the SMPL kinematic structure with $J =$

TABLE I
PERFORMANCE WITH DIFFERENT SAMPLING STRATEGIES

Sampling Strategy		Tracking Task					Perturbation Task	
State	Action	Success (%) \uparrow	$E_{g\text{-mpjpe}} \downarrow$	$E_{\text{mpjpe}} \downarrow$	$E_{\text{vel}} \downarrow$	$E_{\text{acc}} \downarrow$	Success ID (%) \uparrow	FPV \downarrow
Clean	Clean	68.8	57.1	33.1	8.77	5.55	3.36	-
Noisy	Noisy	64.5	61.7	41.4	16.3	17.6	59.5	7.94
Noisy*	Clean*	93.5	49.9	31.6	8.25	5.55	100.0	2.77

TABLE II
MOTION TRACKING RESULTS ON AMASS TRAIN AND TEST DATASETS

AMASS-Train*						AMASS-Test*				
Method	Success (%) \uparrow	$E_{g\text{-mpjpe}} \downarrow$	$E_{\text{mpjpe}} \downarrow$	$E_{\text{vel}} \downarrow$	$E_{\text{acc}} \downarrow$	Success (%) \uparrow	$E_{g\text{-mpjpe}} \downarrow$	$E_{\text{mpjpe}} \downarrow$	$E_{\text{vel}} \downarrow$	$E_{\text{acc}} \downarrow$
MLP	98.8	37.3	26.5	4.6	3.0	97.8	47.3	30.9	8.0	5.9
PHC	98.9	37.5	26.9	4.9	3.3	96.4	47.4	30.9	9.1	6.8
PDP (Ours)	98.9	36.8	26.2	4.7	3.3	97.1	46.2	30.2	8.0	5.7

23 spherical joints. The reference motion includes the linear position $\mathbf{x}_{ref}^p \in \mathbb{R}^{3J}$ and 6d rotation $\mathbf{x}_{ref}^r \in \mathbb{R}^{6J}$ of each joint. The linear and angular velocities are found by finite difference $\dot{\mathbf{x}}_{ref}^p \in \mathbb{R}^{3J}$, $\dot{\mathbf{x}}_{ref}^r \in \mathbb{R}^{6J}$ respectively. The full motion tracking observation can then be defined as a tuple $(\Delta \mathbf{x}^p, \Delta \mathbf{x}^r, \Delta \dot{\mathbf{x}}^p, \Delta \dot{\mathbf{x}}^r, \mathbf{x}_{ref}^p, \mathbf{x}_{ref}^r)$, where $\Delta \mathbf{x}^p = \mathbf{x}_{ref}^p - \mathbf{x}^p$ and the other Δ terms are similarly defined. All quantities are measured in the character frame, where the origin is placed at the root of the character, the x-axis aligns with the character’s facing direction, and the z-axis points upward.

We train PDP with a history of 4 observations and 1 action prediction horizon. For ablation experiments using KIT, we train on 4 *NVIDIA A100* GPUs for approximately 24 hours. For experiments using AMASS, we train on 8 *NVIDIA V100* GPUs for about 70 hours.

C. Text-to-Motion

In the physics-based text-to-motion application, the goal is to train a diffusion policy to generate motions conditioned on a natural language text prompt.

1) *Dataset*: For training data, we use KIT dataset and the text annotations from HumanML3D [9]. The task vector is generated by passing the text annotation through the CLIP embedding [26]. We use the same pre-trained tracking controller, PHC, to obtain the observations and actions for training.

2) *Experimental Details*: The observation space used to train PDP with the text-to-motion task is different from the tracking task. We use the joint position $\mathbf{x}^p \in \mathbb{R}^{3J}$ and linear velocities $\dot{\mathbf{x}}^p \in \mathbb{R}^{3J}$, as well as the joint rotation $\mathbf{x}^r \in \mathbb{R}^{6J}$ and rotational velocities $\dot{\mathbf{x}}^r \in \mathbb{R}^{6J}$. All quantities are measured in the character frame as defined in the motion tracking task. We use a history of 4 observations and 12 action prediction horizon. We train on 4 *NVIDIA A100* GPUs for approximately 32 hours.

V. RESULTS

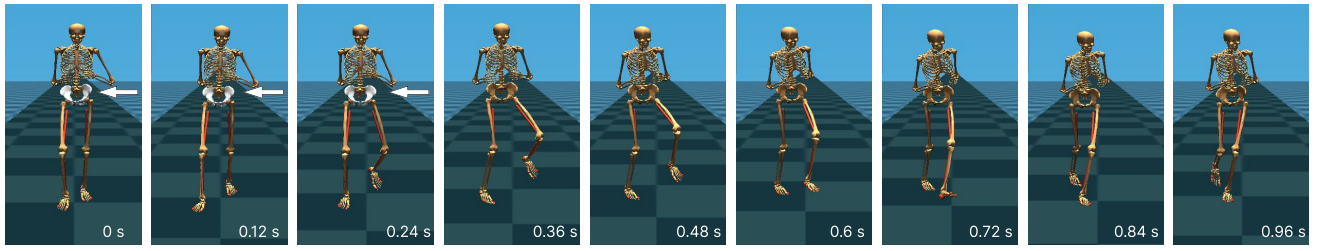
The experiments are designed to answer the following questions.

- 1) Does the proposed sampling strategy, noisy-state-clean-action, outperform alternatives sampling strategies?
- 2) For the application of perturbation recovery during locomotion, can PDP achieve both robust and diverse control policy?
- 3) For universal motion tracking, how does PDP compare to the state-of-the-art RL policy and how important is it to use a generative model for this task?
- 4) Can we train a physics-based text-to-motion policy using PDP?

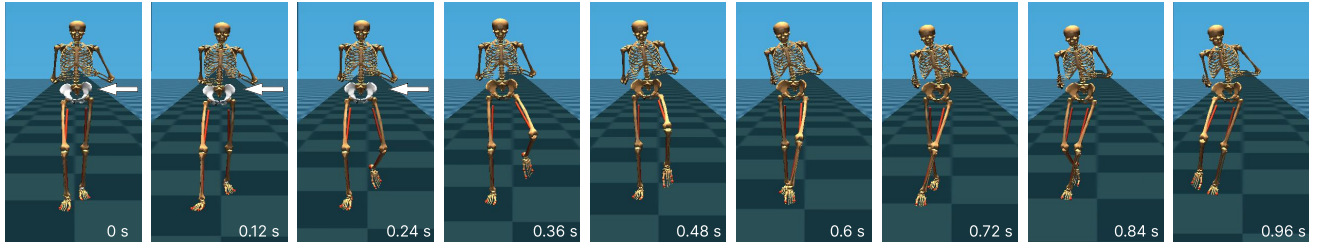
A. Sampling Strategy

We examine the impact of sampling strategies on the tracking and perturbation tasks. For the tracking task, training was conducted using the KIT dataset, with evaluations performed on the test set employed in the AMASS-Test split. Table IV-A2 records the quantitative results of different sampling strategies.

The clean-state clean-action approach has the lowest performance, with a success rate of 3.36% for perturbation and 68.8% for tracking. In comparison, the noisy-state noisy-action strategy significantly improved the perturbation task to 66.9%, but the tracking performance dropped to 64.5%. A possible explanation for the drop in performance in the tracking task but increased performance in the perturbation task is the scale of datasets. The clean-state clean-action strategy restricted the perturbation dataset to just 14 unique trajectories, limiting its diversity. In contrast, the tracking task included 3,626 examples, making it less dependent on additional data from noisy sampling. Thus, random sampling strategies were likely more beneficial for the perturbation task as they introduced necessary variability lacking in the original dataset.

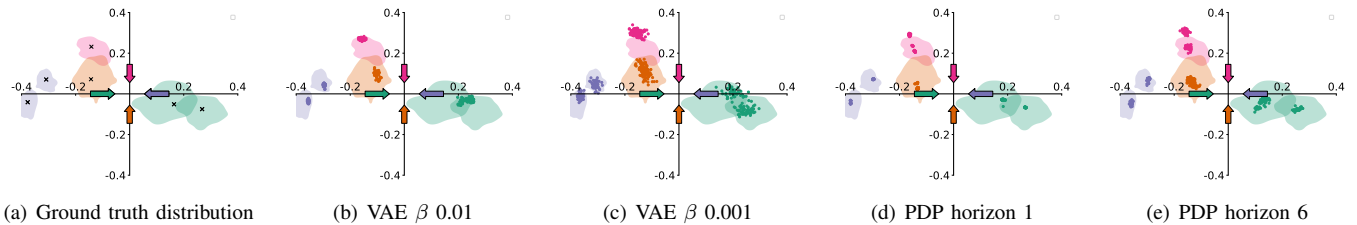


(a)



(b)

Fig. 3. PDP rollouts for a 15% body weight perturbation where the white pelvis and arrows indicate where the force is applied and the direction, respectively. Each row demonstrates a unique mode of recovery from the same perturbation.



(a) Ground truth distribution

(b) VAE β 0.01(c) VAE β 0.001

(d) PDP horizon 1

(e) PDP horizon 6

Fig. 4. Global left foot contact positions after 15% body weight perturbation in meters. +Y and +X align with the character’s forward and right directions, respectively. The different colored arrows represent the directions that the force is applied on the person. The shaded areas represent foot contacts in the training distribution with noise level 0.12. The black X’s represent the ground truth foot contacts of the human participant. All policies were trained on the stochastic dataset with noise level 0.12.

Noisy-state clean-action strategy outperforms other strategies, achieving a perfect success rate of 100% in the perturbation task and 93.5% success rate in the tracking task, see Table IV-A2. These results underscore the importance of selecting the right sampling strategy. By visiting out-of-distribution states and collecting the optimal action, this approach generates higher quality demonstrations, leading to better generalization and robustness.

B. Perturbation Recovery

We compare the performance of PDP to two other baselines, a C-VAE and an MLP. The selection of these approaches was based on their reliance on supervised learning principles. The C-VAE introduces an alternative generative model framework, whereas the MLP serves as a deterministic alternative. The C-VAE uses a similar setup as [18] where state and next state are fed into an encoder to produce a latent code. A decoder takes a randomly sampled latent vector alongside the current state to produce the current action. Both the C-VAE and MLP follow the same architecture as PDP with minor algorithm-dependent adjustments such as excluding the diffusion timestep embedding.

1) *Robustness*: Robustness is measured by the successful completion of an episode, defined as the agent not falling within 6 seconds of the perturbation, a period that allows for several gait cycles to complete post-perturbation. Perturbations are categorized into In-Distribution (ID), which are the same as those in the training data, and Out-of-Distribution (OOD) perturbations, which determines the policy’s capacity to effectively handle unforeseen perturbations by adjusting aspects such as timing, intensity, and direction of impact. We sample OOD perturbations as follows: We choose a random perturbation to cover all gait phases by randomly choosing an impact timing within [0, 2] seconds (equivalent to 2.5 gait cycles overlap), a random force magnitude between 7.5% and 15% of body weight which represents the extrema of the forces used in the Bump-em dataset, and a random force direction that is parallel to the ground.

Table III show the ID and OOD performance of each baseline. All three models can handle ID perturbations, achieving a success rate of 100%. However, when faced with OOD perturbations, C-VAE and PDP methods exhibit notably higher performance, with C-VAE achieving a success rate of 91.3%

and PDP achieving a success rate of 96.3%. Handling OOD impacts is challenging because the model may not have seen them before, especially the impact timing, as all training examples occur at the left toe-off. The OOD distribution performance results could be attributed to the multi-modal nature of the dataset, where using an MLP would result in policies that return the average of the response recorded in the dataset, causing the policy to fail, while C-VAE and PDP can synthesize a more tailored response from the multimodal distribution.

2) *Foot Placement Variability*: Foot placement holds significant importance in understanding perturbation response and balance [32], [33]. A reliable model should ideally mirror the human response or closely approximate it while also accounting for multi-modality. Figure 4a illustrates both the actual foot placements of the participant and the distribution of foot placements obtained through a noisy sampling procedure. When examining foot placement variability for impacts within the distribution, a lower variance in foot placement should be anticipated. This is gauged by assessing the variance in the L2 distance between each foot placement and the nearest ground truth data point. We design a metric based on this called Foot Placement Variability (FPV) to answer how spread apart the foot positions are from the policy compared to the closest ground truth position:

$$FPV = \frac{1}{N} \sum_{i=1}^N \left(\min_{j \in \{1, 2, \dots, M\}} \sqrt{(x_i - \bar{x}_j)^2 + (y_i - \bar{y}_j)^2} \right) \quad (3)$$

where (x_i, y_i) refers to the foot contact position from a single policy rollout and (\bar{x}_j, \bar{y}_j) refers to the ground truth foot contact positions.

PDP achieves a much lower FPV score, 2.79 compared to the top performing C-VAE model $\beta = .001$, 4.97 as shown in Table III, signifying its proficiency in generating action state sequences that closely align with human responses. This is also demonstrated in Figure 4 where it is clear that PDP aligns more closely to the ground truth foot contact positions than the C-VAE.

C-VAE also struggles to capture multi-modality effectively. This is exemplified in the right impact, where the C-VAE prioritizes modeling one mode while PDP is able to generate both modes. Figure 3 shows two responses by the diffusion policy for the rightwards impact. Figure 4 also displays the initial foot contact positions in response to the perturbation from both models. Balancing the reconstruction loss and the KL loss in C-VAE results in a significant trade-off in capturing the multi-modality and the variance in foot contact. Allowing the model to exhibit more variance enables better mode capture. Conversely, reducing the significance of the latent code leads to the model collapsing to a specific response with reduced variance. The comparison between Figure 4b and 4c may seem counter-intuitive in that increasing the β term decreases variability. Nevertheless, this issue of posterior

TABLE III
BASELINE COMPARISONS FOR PERTURBATION TASK

Method	Beta Value	Success ID (%) \uparrow	Success OOD (%) \uparrow	FPV \downarrow
C-VAE	0.0001	98.1	91.0	5.09
	0.001	100.0	91.3	4.97
	0.01	100.0	71.0	4.26
	0.1	99.8	61.3	5.27
	1.0	99.8	59.0	5.28
MLP	-	100.0	81.0	-
PDP	-	100.0	96.3	2.79

TABLE IV
NOISE LEVEL AND HORIZON ABLATION FOR PERTURBATION TASK

Noise Level	Horizon	Success ID (%) \uparrow	Success OOD (%) \uparrow	FPV \downarrow
0.0	6	3.36	0.0	-
0.08	6	97.9	75.0	2.26
0.12	6	100.0	90.0	2.77
0.16	6	90.5	83.0	2.98
0.12	1	100.0	96.3	2.79
0.12	6	100.0	90.0	2.77
0.12	9	65.0	19.7	3.40
0.12	12	6.5	3.6	-

collapse is linked to C-VAE and is further discussed in the Discussion section.

C. Motion Tracking

We demonstrate that PDP is capable of reliably tracking a significant portion of the motion in AMASS. Our method achieves a 96.4% success rate on the AMASS test dataset, where failure is defined as in PHC [14]: an episode is considered a failure if at any point during evaluation the joints are, on average, more than 0.5 meters from the reference motion. In addition to the success rate, we also adopt metrics used by [14], specifically mean per-joint position error (E_{mpjpe}) and global mean per-joint position error ($E_{g-mpjpe}$), which assess the model’s accuracy in matching the reference motion in local and global frames. We also measure the error in velocity (E_{vel}) and acceleration (E_{acc}) between the simulated character and the motion capture data. As shown in Table II, PDP matches or outperforms PHC in all metrics.

Given the same architecture, we also compare with a regression model using MLP without diffusion, and find that MLP outperforms both PDP and PHC. This result is not entirely surprising because the benefit of generative models for the motion tracking application is not obvious in this task, as the action for tracking a particular reference pose from a particular state is not multi-modal but could be used as a motion prior.

D. Text-to-Motion

Figure 1 (middle) shows our results in the text-to-motion domain. We demonstrate that PDP is capable of following diverse text commands in natural language, such as jumping and kicking commands. Evaluating a model that employs auto-regressive inference during simulation with a limited history for composite actions presents significant challenges.

Specifically, a prompt such as “walk then jump” cannot be effectively executed because the agent lacks the necessary memory of the initial action. To address this, we evaluate the model using a set of 42 action text prompts from the dataset, such as “a person dances” and “a person walks forward”. Each prompt is considered successful if the model performs the specified action without falling.

Diffusion models excel in handling multi-modal distributions, which may not significantly benefit the motion tracking task. However, in the text-to-motion application, where capturing multi-modality is crucial, diffusion models (PDP) significantly outperforms MLP achieving a success rate of 57.1% compared to 11.9%, respectively.

VI. DISCUSSION

a) Robust Locomotion Policies: Given the recent robotics community’s interest in developing robust humanoid locomotion policies, our findings are particularly relevant [34]–[36]. While a single optimal strategy might suffice for a specific impact or perturbation, our results indicate that an MLP, which cannot capture different modes, lacks robustness to out-of-distribution (OOD) perturbations. In contrast, our diffusion model effectively stores a variety of strategies, providing it with a broader base of information to draw from when an OOD impact occurs. This capability could enhance locomotion policies’ ability to handle diverse and unpredictable real-world perturbations.

b) C-VAE Posterior Collapse in Perturbation Recovery Task: Tuning the Beta value in C-VAE models presents significant challenges, primarily due to the posterior collapse problem. Increasing the β value forces the latent distribution to align more closely with a normal distribution and can cause the model to disregard the latent vector and rely solely on the observation, effectively reducing the model to function like an MLP. We find that diffusion models cover the distribution of initial foot contact positions more effectively while requiring less tuning, making this model a preferred choice.

c) PDP and MLP Tracking Task: Previous literature has shown the difficulty of producing a single and reliable motion tracker [14], [37]. Our method can train a model directly through supervised learning and exceed the performance of more complex hierarchical RL policies. Furthermore, This capability facilitates the creation of a pre-trained tracking controller that can be swiftly adapted to new datasets. This feature is notably distinct from conventional RL-based methods [13], [14] which necessitates retraining or fine-tuning controllers. Our method requires only a few noisy rollouts and a few epochs of additional learning to obtain new skills. Given the small data volume, this process is relatively quick, taking only a few minutes excluding the training of the expert policy.

d) Text2Motion Challenges: Our system’s capability extends to the text-to-motion task, demonstrating smooth transitions between text prompts despite a limited range of transitions. We hypothesize this effectiveness is partly due to the noisy sampling approach. By creating a band around each clean trajectory, we inadvertently increase the likelihood of

intersecting with the state of another motion, facilitating more transitions.

However, our empirical observations indicate that text-to-motion does not perform at the same level as kinematic motion generation models. This discrepancy can likely be attributed to several factors. First, the model must balance performing the motion and maintaining equilibrium. When losing balance, it compensates with small corrective steps, disrupting the original motion. Secondly, while combining two distinct motions can be close in kinematic space, like superimposing root rotation onto a jump to create a jump-and-turn motion, achieving these motions may be significantly different in skill space. That is, the agent faces a challenge in determining how to manipulate the feet to rotate the root while simultaneously executing the jump.

e) Limitations: Despite its advantages, our approach has notable limitations. The primary constraint is the speed of the denoising process. It is significantly slower than a single forward pass of a typical MLP, making it challenging for real-time motion tracking applications. However, recent works such as [4], [38] offer promising avenues for speeding up this process.

VII. CONCLUSION AND FUTURE WORK

We present a novel framework for physics-based character control that leverages the capability of diffusion models to capture diverse behaviors. Our proposed sampling strategy, noisy-state-clean-action, significantly outperforms alternative sampling strategies. For the perturbation recovery task, our method effectively captures the distribution of human responses and demonstrates robustness to both in-distribution and out-of-distribution perturbations. In universal motion tracking, our method surpasses the state-of-the-art performance, including our baseline using a non standard non-generative model. Additionally, we showcase our methods ability to synthesize motion conditioned on text. Future work could look into speeding up the inference by using methods like [38], [39], or leveraging the large pre-trained motion tracker for downstream RL tasks.

REFERENCES

- [1] G. Tevet, S. Raab, B. Gordon, Y. Shafir, D. Cohen-or, and A. H. Bermano, “Human motion diffusion model,” in *The Eleventh International Conference on Learning Representations*, 2023. [Online]. Available: <https://openreview.net/forum?id=SJ1kSyO2jwu>
- [2] J. Tseng, R. Castellon, and C. K. Liu, “Edge: Editable dance generation from music,” 2022.
- [3] C. Chi, S. Feng, Y. Du, Z. Xu, E. Cousineau, B. Burchfiel, and S. Song, “Diffusion policy: Visuomotor policy learning via action diffusion,” in *Proceedings of Robotics: Science and Systems (RSS)*, 2023.
- [4] X. Huang, Y. Chi, R. Wang, Z. Li, X. B. Peng, S. Shao, B. Nikolic, and K. Sreenath, “Diffuseloco: Real-time legged locomotion control with diffusion from offline datasets,” 2024.
- [5] Y. Song and S. Ermon, “Improved techniques for training score-based generative models,” *CoRR*, vol. abs/2006.09011, 2020. [Online]. Available: <https://arxiv.org/abs/2006.09011>
- [6] Z. Xie, P. Clary, J. Dao, P. Morais, J. Hurst, and M. Panne, “Learning locomotion skills for cassie: Iterative design and sim-to-real,” in *Conference on Robot Learning*. PMLR, 2020, pp. 317–329.

- [7] K. Werling, N. A. Bianco, M. Raitor, J. Stingel, J. L. Hicks, S. H. Collins, S. L. Delp, and C. K. Liu, "Addbiomechanics: Automating model scaling, inverse kinematics, and inverse dynamics from human motion data through sequential optimization," *Plos one*, vol. 18, no. 11, p. e0295152, 2023.
- [8] N. Mahmood, N. Ghorbani, N. F. Troje, G. Pons-Moll, and M. J. Black, "AMASS: Archive of motion capture as surface shapes," in *International Conference on Computer Vision*, Oct. 2019, pp. 5442–5451.
- [9] C. Guo, S. Zou, X. Zuo, S. Wang, W. Ji, X. Li, and L. Cheng, "Generating diverse and natural 3d human motions from text," in *Proceedings of the IEEE/CVF Conference on Computer Vision and Pattern Recognition (CVPR)*, June 2022, pp. 5152–5161.
- [10] X. B. Peng, P. Abbeel, S. Levine, and M. van de Panne, "Deepmimic: Example-guided deep reinforcement learning of physics-based character skills," *ACM Trans. Graph.*, vol. 37, no. 4, pp. 143:1–143:14, Jul. 2018. [Online]. Available: <http://doi.acm.org/10.1145/3197517.3201311>
- [11] K. Bergamin, S. Clavet, D. Holden, and J. R. Forbes, "Drecon: data-driven responsive control of physics-based characters," *ACM Transactions On Graphics (TOG)*, vol. 38, no. 6, pp. 1–11, 2019.
- [12] S. Park, H. Ryu, S. Lee, S. Lee, and J. Lee, "Learning predict-and-simulate policies from unorganized human motion data," *ACM Transactions on Graphics (TOG)*, vol. 38, no. 6, pp. 1–11, 2019.
- [13] J. Won, D. Gopinath, and J. Hodgins, "A scalable approach to control diverse behaviors for physically simulated characters," *ACM Transactions on Graphics (TOG)*, vol. 39, no. 4, pp. 33–1, 2020.
- [14] Z. Luo, J. Cao, A. Winkler, K. Kitani, and W. Xu, "Perpetual humanoid control for real-time simulated avatars," 2023.
- [15] X. B. Peng, Z. Ma, P. Abbeel, S. Levine, and A. Kanazawa, "AMP: adversarial motion priors for stylized physics-based character control," *CoRR*, vol. abs/2104.02180, 2021. [Online]. Available: <https://arxiv.org/abs/2104.02180>
- [16] H. Yao, Z. Song, Y. Zhou, T. Ao, B. Chen, and L. Liu, "Moconvq: Unified physics-based motion control via scalable discrete representations," *arXiv preprint arXiv:2310.10198*, 2023.
- [17] Q. Zhu, H. Zhang, M. Lan, and L. Han, "Neural categorical priors for physics-based character control," *ACM Transactions on Graphics (TOG)*, vol. 42, no. 6, pp. 1–16, 2023.
- [18] J. Won, D. Gopinath, and J. Hodgins, "Physics-based character controllers using conditional vaes," *ACM Trans. Graph.*, vol. 41, no. 4, jul 2022. [Online]. Available: <https://doi.org/10.1145/3528223.3530067>
- [19] J. Merel, L. Hasenclever, A. Galashov, A. Ahuja, V. Pham, G. Wayne, Y. W. Teh, and N. Heess, "Neural probabilistic motor primitives for humanoid control," *arXiv preprint arXiv:1811.11711*, 2018.
- [20] X. B. Peng, Y. Guo, L. Halper, S. Levine, and S. Fidler, "Ase: Large-scale reusable adversarial skill embeddings for physically simulated characters," *ACM Transactions On Graphics (TOG)*, vol. 41, no. 4, pp. 1–17, 2022.
- [21] J. Tseng, R. Castellon, and K. Liu, "Edge: Editable dance generation from music," in *Proceedings of the IEEE/CVF Conference on Computer Vision and Pattern Recognition*, 2023, pp. 448–458.
- [22] E. Ng, Z. Liu, and M. Kennedy, "Diffusion co-policy for synergistic human-robot collaborative tasks," *IEEE Robotics and Automation Letters*, vol. 9, no. 1, pp. 215–222, 2024.
- [23] E. Zhang, Y. Lu, W. Y. Wang, and A. Zhang, "Lad: Language augmented diffusion for reinforcement learning," in *Second Workshop on Language and Reinforcement Learning*, 2022.
- [24] J. Ho, A. Jain, and P. Abbeel, "Denoising diffusion probabilistic models," *CoRR*, vol. abs/2006.11239, 2020. [Online]. Available: <https://arxiv.org/abs/2006.11239>
- [25] M. Welling and Y. W. Teh, "Bayesian learning via stochastic gradient langevin dynamics," in *Proceedings of the 28th international conference on machine learning (ICML-11)*, 2011, pp. 681–688.
- [26] A. Radford, J. W. Kim, C. Hallacy, A. Ramesh, G. Goh, S. Agarwal, G. Sastry, A. Askell, P. Mishkin, J. Clark, G. Krueger, and I. Sutskever, "Learning transferable visual models from natural language supervision," *CoRR*, vol. abs/2103.00020, 2021. [Online]. Available: <https://arxiv.org/abs/2103.00020>
- [27] E. Perez, F. Strub, H. de Vries, V. Dumoulin, and A. C. Courville, "Film: Visual reasoning with a general conditioning layer," *CoRR*, vol. abs/1709.07871, 2017. [Online]. Available: <http://arxiv.org/abs/1709.07871>
- [28] A. Jensen, T. Chatagnon, N. Khoshshiyar, D. Reda, M. Van De Panne, C. Pontonnier, and J. Pettré, "Physical simulation of balance recovery after a push," in *Proceedings of the 16th ACM SIGGRAPH Conference on Motion, Interaction and Games*, ser. MIG '23. New York, NY, USA: Association for Computing Machinery, 2023. [Online]. Available: <https://doi.org/10.1145/3623264.3624448>
- [29] B. K. Hodossy and D. Farina, "Shared autonomy locomotion synthesis with a virtual powered prosthetic ankle," *IEEE Transactions on Neural Systems and Rehabilitation Engineering*, vol. 31, pp. 4738–4748, 2023.
- [30] G. R. Tan, M. Raitor, and S. H. Collins, "Bump'em: an open-source, bump-emulation system for studying human balance and gait," in *2020 IEEE International Conference on Robotics and Automation (ICRA)*, 2020, pp. 9093–9099.
- [31] M. Plappert, C. Mandery, and T. Asfour, "The kit motion-language dataset," *Big data*, vol. 4, no. 4, pp. 236–252, 2016.
- [32] J. A. Perry and M. Srinivasan, "Walking with wider steps changes foot placement control, increases kinematic variability and does not improve linear stability," *Royal Society open science*, vol. 4, no. 9, p. 160627, 2017.
- [33] J. R. Rebula, L. V. Ojeda, P. G. Adamczyk, and A. D. Kuo, "Measurement of foot placement and its variability with inertial sensors," *Gait & posture*, vol. 38, no. 4, pp. 974–980, 2013.
- [34] Ç. Kaymak, A. Uçar, and C. Güzeliş, "Development of a new robust stable walking algorithm for a humanoid robot using deep reinforcement learning with multi-sensor data fusion," *Electronics*, vol. 12, no. 3, p. 568, 2023.
- [35] Z. Li, X. Cheng, X. B. Peng, P. Abbeel, S. Levine, G. Berseth, and K. Sreenath, "Reinforcement learning for robust parameterized locomotion control of bipedal robots," in *2021 IEEE International Conference on Robotics and Automation (ICRA)*. IEEE, 2021, pp. 2811–2817.
- [36] R. P. Singh, Z. Xie, P. Gergondet, and F. Kanehiro, "Learning bipedal walking for humanoids with current feedback," *IEEE Access*, 2023.
- [37] J. Won, D. Gopinath, and J. Hodgins, "A scalable approach to control diverse behaviors for physically simulated characters," *ACM Trans. Graph.*, vol. 39, no. 4, aug 2020. [Online]. Available: <https://doi.org/10.1145/3386569.3392381>
- [38] T. Yin, M. Gharbi, R. Zhang, E. Shechtman, F. Durand, W. T. Freeman, and T. Park, "One-step diffusion with distribution matching distillation," 2023.
- [39] A. Gu and T. Dao, "Mamba: Linear-time sequence modeling with selective state spaces," 2023.